Fiedler, B., Hainzl, S., Zöller, G., Holschneider, M. (2018): Detection of Gutenberg–Richter b-Value Changes in Earthquake Time Series. - *Bulletin of the Seismological Society of America*, *108*, 5A, pp. 2778—2787.

DOI: http://doi.org/10.1785/0120180091

Detection of Gutenberg-Richter b-value changes in earthquake time series

August 28, 2018

Bernhard Fiedler, Institute of Mathematics, University of Potsdam, Karl-Liebknecht-Str. 24-25, 14476 Potsdam, Germany. Email bfiedler@uni-potsdam.de

Sebastian Hainzl, GFZ German Research Centre for Geosciences, Telegrafenberg, 14473 Potsdam, Germany

Gert Zöller, Institute of Mathematics, University of Potsdam, Karl-Liebknecht-Str. 24-25, 14476 Potsdam, Germany

Matthias Holschneider, Institute of Mathematics, University of Potsdam, Karl-Liebknecht-Str. 24-25, 14476 Potsdam, Germany

Abstract

The Gutenberg-Richter relation for earthquake magnitudes is the most famous empirical law in seismology. It states that the frequency of earthquake magnitudes follows an exponential distribution, which is found to be a robust feature of seismicity above the completeness magnitude, independent whether global, regional, or local seismicity is analyzed. However, the exponent b of the distribution varies significantly in space and time which is important for process understanding and seismic hazard assessment; particularly because the Gutenberg-Richter b-value acts as proxy for the stress state and quantifies the ratio of large to small earthquakes. In our work we focus on the automatic detection of statistically significant temporal changes of the b-value in seismicity data. In our approach, we use Bayes factors for model selection and estimate multiple change-points of the frequency-magnitude distribution in time. The method is first applied to synthetic data showing its capability to detect change-points as function of the size of the sample and the b-value contrast. Finally, we apply this approach to examples of observational data sets for which previously b-value changes have been stated. Our analysis of foreshock- and aftershock sequences related to mainshocks, as well as earthquake swarms, shows that only a part of the b-value changes is found to be statistically significant.

Introduction

The frequency of earthquake magnitudes m is usually well described by the Gutenberg-Richter relation

$$\log N(M) = a - bM, \quad M \geq M_c, \tag{1}$$

which declares that the number of earthquakes N with magnitude equal or greater than M decreases exponentially with M (Gutenberg and Richter, 1956). Here the lower cutoff M_c refers to the magnitude of completeness, i.e. all events $M \geq M_c$ are assumed to be recorded in the given catalog. The a-value describes the overall seismicity level in the region of interest. The Gutenberg-Richter b-value determines the ratio between large to small events, e.g. a b-value equal to one means that there are ten times more events with magnitude $M = 2$ than with magnitude $M = 3$. For $b < 1$, high magnitude events are more frequent, whereas $b > 1$ implies more small events. Thus the b-value is one of the key parameters for seismic hazard estimations.

For the whole Earth or catalogs containing a huge number of events and covering a large area, the b-value is usually approximately one. Nevertheless strong local variations are reported with typical ranges $0.4 < b < 2.0$ (Wiemer and Wyss, 2002). Laboratory experiments have shown that the b-value describing the size distribution of acoustic emission events decreases with differential stress (Scholz, 1968; Amitrano, 2003; Goebel et al., 2013) which seems to be in agreement with observations for earthquakes (Schorlemmer et al., 2005; Spada et al., 2013; Scholz, 2015). Therefore many studies suggested that temporal b-value changes might be precursory signals which can be useful for forecasting mainshocks, as e.g. (Smith, 1981; Imoto, 1991; Nakaya, 2006; Nanjo et al., 2012). However, the statistical significance of such observed variations might be questionable, due to statistical fluctuations of limited sample sizes and binned data (Kamer and Hiemer, 2013).

In our work, we therefore develop a Bayesian approach to detect statistically significant temporal changes of the frequency-magnitude distribution without any predefined binning of the data (see Section *Method*). For this purpose, we adapt a multiple change-point estimator recently developed for detecting seismicity rate changes (Fiedler et al., 2018). In an iterative approach, we use the Bayes factor for deciding whether or not change-points exist and estimate the change-points where required. The method is first applied to synthetic data showing its capability to detect real change-points (Section *Test for synthetic data*). As examples, we finally apply this approach to fore- and aftershock sequences as well as to swarm activity for which b-value changes have been previously claimed (Section *Application to observations*).

Method

In the case of an unbounded Gutenberg-Richter model, the probability density function for magnitudes $M \geq M_c$ reads

$$f_{M_c\beta}(M) = \beta \exp\left[-\beta(M - M_c)\right], \tag{2}$$

where $\beta = \ln(10)b$ represents the Gutenberg-Richter b-value. We assume that the completeness magnitude M_c is known for the given region. For simplicity, we consider in the following only the variable, $m = M - M_c$, which is the difference between the event magnitude and the completeness magnitude. Note that M_c can vary in space and time. This leads to

$$f_\beta(m) = \beta \exp(-\beta m), \quad m \geq 0. \tag{3}$$

Although the b-value is an unknown parameter to be estimated, some prior knowledge can be assumed. Estimated b-values for natural seismicity are usually less than 2 (Wiemer and Wyss, 2002), while b-values up to 3 have been sometimes also reported for induced seismicity (Bachmann et al., 2012; Lopez-Comino et al., 2017). Thus the overall b-value range can be assumed to be $[0, 3]$.

In our study we consider an observation period of $[T_0,\ T_1]$ with N events at times $T_0 \leq t_1 < t_2 < \ldots < t_N \leq T_1$. Here m_i is the magnitude occurring at time t_i, $i = 1, \ldots, N$. We assume the existence of one change-point after the kth observation ($k = 1, \ldots, N-1$). Thus we have k events with β_1 in $[T_0,\ t_k]$ and $N-k$ events with β_2 in $(t_k,\ T_1]$.

Let $\underline{m} = \{m_1, \ldots, m_N\}$ and $\theta = \{\beta_1,\ \beta_2,\ k\}$. It can easily be shown that the mutual likelihood function is given by

$$p(\underline{m} \mid \theta) = \beta_1^k \exp\left(-\beta_1 \sum_{i=1}^{k} m_i\right) \beta_2^{N-k} \exp\left(-\beta_2 \sum_{l=k+1}^{N} m_l\right). \tag{4}$$

In the case of no change-point the likelihood function reads as

$$p(\underline{m} \mid \beta_0) = \beta_0^N \exp\left(-\beta_0 \sum_{i=1}^{N} m_i\right). \tag{5}$$

Let $p(\beta_i)$ denote the prior density for β_i with $i = 0, 1, 2$ and $p(k)$ the prior density for the change-point index k. Assuming a priori independence of β_1, β_2 and k and using Bayes theorem, we get the posterior densities

$$p(\theta \mid \underline{m}) \propto p(\beta_1)p(\beta_2)p(k)\beta_1^k \exp\left(-\beta_1 \sum_{i=1}^{k} m_i\right) \beta_2^{N-k} \exp\left(-\beta_2 \sum_{i=k+1}^{N} m_i\right) \quad (6)$$

and

$$p(\beta_0 \mid \underline{m}) \propto p(\beta_0)\beta_0^N \exp\left(-\beta_0 \sum_{i=1}^{N} m_i\right). \quad (7)$$

In the following we use Eq. (6) and Eq. (7) for the calculation of the Bayes factors to determine whether or not change-points exist and then for the estimation of the (possible) change-points; i.e. in our approach we first select a suitable model and then estimate the position of the change-points.

Model selection

First we give a brief overview on the calculation of the Bayes factor which is defined by the ratio of the marginal or integrated likelihood for the two considered models. In our study $\mathcal{M}_0$ is a model without a change-point and $\mathcal{M}_1$ a model with one change-point, i.e.

$$B_{01} = \frac{p(\underline{m} \mid \mathcal{M}_0)}{p(\underline{m} \mid \mathcal{M}_1)}. \quad (8)$$

Apart from the goodness of fit, the complexity of the assumed model has to be taken into account in order to assess the most capable model describing the data and thus performing the estimation. The value of the Bayes factor quantifies the evidence of the supported model, e.g. small values for B_{01} can be interpreted as a decisive evidence against the hypothesis of no change-point ($\mathcal{H}_0$), compare Kass and Raftery (1995). We remark that Eq. (8) depends on the choice of the priors. Unfortunately it is not well-defined for improper priors due to the marginalization paradox (Dawid et al., 1973). From Eq. (6) and Eq. (7) we get

$$p(\underline{m} \mid \mathcal{M}_0) = \int_0^\infty p(\beta)\beta^N \exp\left(-\beta \sum_{i=1}^{N} m_i\right) d\beta \tag{9}$$

and

$$\begin{aligned} p(\underline{m} \mid \mathcal{M}_1) = \sum_{k=1}^{N-1} \int_0^\infty \int_0^\infty & p(k)p(\beta_1)p(\beta_2)\beta_1^k \exp\left(-\beta_1 \sum_{i=1}^{k} m_i\right) \\ & \times \beta_2^{N-k} \exp\left(-\beta_2 \sum_{i=k+1}^{N} m_i\right) d\beta_1\, d\beta_2. \end{aligned} \tag{10}$$

In the following we assume a uniform prior density for the Gutenberg-Richter b-values in the domain $[0, \beta_{max}]$, where β_{max} denotes the upper cutoff, and we use a discrete uniformly distributed prior for k, i.e. $p(k) = \frac{1}{N-1}$. It is shown in the Appendix *Derivation of the Bayes factor* that the evaluation of Eq. (9) and Eq. (10) results in a Bayes factor B_{01} given by

$$B_{01} = \frac{\beta_{max}(N-1)\left[\sum_{i=1}^{N} m_i\right]^{-(N+1)} \gamma\left(N+1, \beta_{max} \sum_{i=1}^{N} m_i\right)}{\sum_{k=1}^{N-1}\left\{\left[\sum_{i=1}^{k} m_i\right]^{-(k+1)} \gamma\left(k+1, \beta_{max}\sum_{i=1}^{k} m_i\right)\left[\sum_{i=k+1}^{N} m_i\right]^{-(N-k+1)} \gamma\left(N-k+1, \beta_{max} \sum_{i=k+1}^{N} m_i\right)\right\}} \tag{11}$$

where γ denotes the incomplete gamma function (see Eq. A2).

Estimation of change-points

To estimate the location k of a change-point, we follow the approach of Raftery and Akman (1986) and Fiedler et al. (2018). The marginal posterior of k is calculated by integrating Eq. (6) with respect to β_1 and β_2. Assuming uniformly distributed prior densities for the parameters $\beta_1,\ \beta_2$ and k (compare Section *Model selection*), we get

$$
\begin{aligned}
p(k \mid \underline{m}) \propto \frac{\beta_{max}^{-2}}{N-1} \int\limits_0^{\beta_{max}} \int\limits_0^{\beta_{max}} \beta_1^k \exp\left(-\beta_1 \sum_{i=1}^{k} m_i\right) \beta_2^{N-k} \exp\left(-\beta_2 \sum_{i=k+1}^{N} m_i\right) d\beta_1\, d\beta_2 \\
= \frac{\beta_{max}^{-2}}{N-1} \left\{ \left[\sum_{i=1}^{k} m_i\right]^{-(k+1)} \gamma\left(k+1, \beta_{max} \sum_{i=1}^{k} m_i\right) \right. \\
\times \left. \left[\sum_{i=k+1}^{N} m_i\right]^{-(N-k+1)} \gamma\left(N-k+1, \beta_{max} \sum_{i=k+1}^{N} m_i\right) \right\}.
\end{aligned}
\tag{12}
$$

By maximizing Eq. (12) with respect to k we obtain the estimation $\hat{k}$ for the change-point index.

Multiple change-points

In the previous subsections, we illustrated a method for the estimation of a single change-point and a foregoing model selection. This leads to the question how to handle a data set with several change-points. Therefore two different approaches are possible. On the one hand an extension of the existing methodology (compare with multiple change-point detection methods for seismicity rates e.g. in Fiedler et al. (2018) or Montoya and Wang (2017)) and on the other hand an iterative algorithm.The calculation of Bayes-factors for multiple change-points becomes quickly very costly, because the computation time scales until N^n with the number n of change-points. As an example, we provide the Bayes factor for two change-points in the Appendix *Derivation of Bayes-factors* and we also show an approach to estimate a fixed number of change-points (see Appendix *Estimation of multiple change-points*). However, based on tests (see Section *Test for synthetic data*) we find that an iterative algorithm is at least as good as an algorithm based on higher order Bayes factors for model selection and reduces the numerical complexity significantly. For the iterative method we use the following greedy algorithm:

i) Consider a data set $[T_0, T_1]$ with N events at $T_0 \leq t_1 < t_2 < \ldots < t_N \leq T_1$.

ii) Calculate the Bayes factor B_{01} (Eq. 11) for the investigated data set.

iii) If the calculated Bayes factor is greater than 0.5, the model without a change-point is selected. Otherwise estimate the change-point index $\hat{k}$ by means of maximizing Eq. (12).

iv) If $B_{01} < 0.5$, set $\tilde{T}_1 = t_{\hat{k}}$, $N_1 = \hat{k}$, $\tilde{T}_0 = t_{\hat{k}+1}$ and $N_2 = N - \hat{k}$ and go to step i) for both resulting subsets $[T_0, \tilde{T}_1]$ with N_1 events and $[\tilde{T}_0, T_1]$ with N_2 events, independently.

In each of the intervals between identified change-points as well as before the first and after the last one, the b-value is then estimated by the maximum likelihood value (Aki, 1965; Marzocchi and Sandri, 2003)

$$\hat{b} = \frac{1}{\ln(10)(\bar{m} + 0.5\Delta m)} \tag{13}$$

with the corresponding estimated standard deviation $\hat{b}/\sqrt{N}$. Here N is the number of events, $\bar{m}$ is the mean value of m, and Δm represents the binning interval of reported magnitudes which is typically 0.01 or 0.1 for real catalogs.

Evaluation and application

The derived methodology from the previous section is for test and illustration purposes firstly applied to synthetic data. Subsequently, it is then applied to six exemplary observed data sets. According to prior observations that the b-value typically ranges from 0 to 3 (see Section *Method*) and our test results (see Section *Test for synthetic data*), we set in all cases the cutoff value $\beta_{max} = 3\ln(10) \approx 6.9$.

Test for synthetic data

We firstly analyze whether 0.5 as threshold of the Bayes-factor is appropriate to discriminate between real changes and random fluctuations. For this purpose, we generate sequences of N events with magnitudes taken from Eq. (3) with constant b-value. For given N and b, we analyze the Bayes factor for 1000 random sequences. We count the number N_0 of cases with $B < 0.5$ and estimate the error probability by $N_0/1000$. This procedure is repeated for b-values in the range between 0.8 and 1.2 and event sizes N between 10 and 5000. Figure **1** shows that the resulting estimated probabilities are independent of b with values below 0.08. The values systematically decrease for increasing N, where largest values are found for smallest samples sizes. For sample sizes around 100, the values scatter around the desired value of 0.05.

In a next step, we analyze the detectability of change-points as function of the sample size and the b-value contrast. For this aim, we generate synthetic time series with a single change-point at the center of the sequence. The first $N/2$ events were randomly chosen from Eq. 2 with a b-value of b_1 and the second half with b_2, where the mean b-value is 1. For a given b-value contrast $\Delta b = b_2 - b_1$ and given sample size N, we generate 10,000 sequences and count the number of cases N_0 when a change-point is detected, i.e. when $B_{01} < 0.5$. The probability to detect the change-point is estimated by the fraction N_0/N. The result is shown as contour lines in Figure **2a** for Δb between 0 and 1 and N between 10 and 10,000. It is found that it is almost impossible to detect a moderate b-value change in sequences with less than 100 events. For example in the case of $N = 100$, a step of $\Delta b = 0.5$ is only detected with statistical significance in half of the sequences. This situation improves significantly for $N = 1000$, when already a change of $\Delta b = 0.2$ is detectable in 50% of the cases. Finally, a small change of $\Delta b = 0.1$ is only detectable in big data sets consisting of approximately 10,000 events or more.

The same testing environment is used to investigate the goodness of the estimated position $\hat{k}$ of the change-point within the sequence of length N. For that purpose, we calculate the root-mean-square (rms) of the relative position $\hat{k}/N$ for those cases with $B_{01} < 0.5$. The result is shown in Figure **2b** as function of Δb and N. High precision is only found for larger Δb- and N-values.

Furthermore we analyze the sensitivity of our method with respect to the choice of the prior distribution. Due to the fact that we have a uniformly distributed prior in the range $[0, b_{max}]$ with $b_{max} = \beta_{max}/\ln(10)$, we investigate the detectability and the precision of the change-point depending on the upper interval limit b_{max}. Therefore we investigate a range from 1.5 to 4.5 for this value. Using the same methodology as shown in Figure **2**, we show the results for three alternative values of Δb with $N = 1000$ and generate 10,000 sequences for every parameter set. As illustrated in Figure **3**, we only have a relatively weak dependency indicating that the main features are rather robust with regard to the choice of b_{max}. The root-mean-square error of the relative position of detected change-points remains almost constant (see Figure **3b**). Nevertheless it is obvious that the detectability is slightly decreasing with increasing b_{max} (compare Figure **3a**). Taking into account that Gutenberg-Richter b-values are usually less than three and that the loss of quality with respect to the detectability also for higher b-values is acceptable, we conclude that the choice of $b_{max} = 3$ is a good compromise for the a priori distribution.

In a last test setup, we show a comparison of the results of our change-point detection method for four different cases with 0, 1, 2, or 12 change-points, respectively. In each case, we apply the method for 100 random sequences with a predefined b-value history. The magnitude versus time plot of one of these sequences is shown on top of each subplot in Figure **4**. Some magnitude trends are visible but its significance is difficult to quantify by eye. The b-value histories reconstructed by our method are shown as gray lines for each of the 100 sequences on bottom of the subplots. These results can be compared to the true values which are shown as red lines in the same plots. We find that the reconstruction overall works well. In all cases, the estimated values scatter around the true ones, even for the quasi-continuous b-value increase in Figure **4d**. For the case with 0, 1, and 2 change-points, we can compare our iterative procedure described in Section *Multiple change-points*, with the computationally more demanding calculation where $B_{12} < 0.5$ is used for deciding for two change-points, if $B_{01} < 0.5$. If yes, the two change-points are calculated simultaneously within the whole sequence. While this procedure takes significantly more computation time, the results, which are shown by blue curves in Figure **4**, indicate no improvement compared to the more efficient iterative procedure.

Application to observations

We now apply the method to real earthquake data, where b-value changes have been previously reported. These sequences comprise two foreshock sequences and two aftershock sequences related to well-known mainshocks in Chile, US, and Japan, as well as two earthquake swarms in Czech Republic. Our goal is to show exemplary applications for estimations of statistical significant b-value changes without detailed physical interpretation.

Foreshock activity

Some of the major earthquakes are preceded by foreshock activity. The detection of particular features of these foreshocks, such as an anomalous b-value, would therefore offer a possibility to improve forecast abilities. Here we analyze two sequences which have been previously shown to have systematic precursory trends of the b-value.

Iquique foreshock activity: On 1 April 2014, Northern Chile was struck by a magnitude 8.1 earthquake following a protracted series of foreshocks. Besides accelerated foreshock activity, Schurr et al. (2014) found that the mainshock area was characterized by low b-values of the foreshock activity and that the b-value decreased prior to the event. We use the same data set to check the significance of this b-value decrease. The data set consists of 1107 foreshocks with $M \geq 3$ occurred between latitude 19°S and 21°S and between longitude -72° and -70° in the 2000 days preceding the mainshock. As shown in Figure **5a**, we find no statistically significant change-points, while the b-value calculations in moving windows of 200 subsequent events suggests some systematic decrease. However, the b-value change is only of the order of 0.2. According to our synthetic test, a change-point with $\Delta b = 0.2$ can be detected in a data set of approximately 1000 events only in less than half of the cases (see Figure **2a**). Thus a b-value decrease might have occurred in this case, but the statistical significance is not clear.

Tohoku foreshock sequence: The destructive 11 March 2011 M_w9.0 Tohoku earthquake was also found retrospectively to be preceded by a systematic decrease of the b-value of foreshocks in the source region (Nanjo et al., 2012). Here we use the Japan Meteorological Agency (JMA) earthquake catalog and select the $M \geq 3$, which should be complete according to Nanjo et al. (2012), within latitude 37.7°N and 39.0°N and longitude 142.7° and 144.0° in the 4000 days preceding the mainshock. The sample consists of 643 foreshocks. The application of the change-point estimation approach results in the detection of one change around 1000 days before the mainshock, when the b-value drops from approximately 0.66 to 0.44 (see Figure **5b**). This is in agreement with the previously observed decreasing trend. However, the continuous decrease suggested by the moving-window approach might be only a smearing effect of the constantly high b-value before 2000 days and a low b-value in the last three years prior to the mainshock, because of the low seismicity in-between.

Aftershock sequences

Aftershocks are triggered by almost every larger earthquake in the vicinity of its rupture. The rate of these aftershocks usually decays in time according to the Omori-Utsu law, $R(t) \sim (c+t)^{-p}$ (Utsu et al., 1995). While the exponent p is typically around 1 and almost independent of the mainshock magnitude, the c-value has been found to strongly depend on the mainshock magnitude (Shcherbakov et al., 2004). However, it has been recognized that earthquake catalogs are incomplete during periods of high activity, particularly in the first period after mainshocks (Kagan, 2004; Hainzl, 2016a), which leads to an apparent low b-value which recovers with time and a c-value which depends on the mainshock magnitude (Hainzl, 2016b). In the following, we demonstrate that data incompleteness can result in artificial change-points. For this goal, we do not correct for completeness immediately after large events.

Landers aftershock sequence: The first analyzed example of such an aftershock sequence is the sequence triggered of the well- known M7.3 Landers, California, mainshock occurred in 1992. We use the relocated earthquake catalog provided by the Southern California Earthquake Data Center (SCEC) (Hauksson et al., 2012) and select $M \geq 2$ events occurred within the first 1000 days after the mainshock within latitude 33.25°N and 35.5°N and longitude -117.5° and -115.5°. The application of our approach for these 15,800 selected aftershocks reveals 5 significant change-points and a systematic increase of the b-value from 0.25 to 1.2 within the first 12 days, while the b-value remains constant for the remaining time (see Figure **5c**).

Tohoku aftershock sequence: The second example stems from the aftershock activity triggered by the 11 March 2011 M9.0 Tohoku. In contrast to the foreshock activity analyzed above for this event, the aftershocks are less concentrated around the hypocenter of the mainshock and we select therefore the $M \geq 3$ aftershocks occurred within the wider region between latitude 35.0°N and 40.0°N and longitude 141° and 144.0° which leads to nearly 20,000 selected events within the first year after the mainshock. Our method also reveals in this case 5 significant change-points of the frequency-magnitude distribution and a systematic increase of the b-value from 0.20 to 0.85 within the first 80 days (see Figure **5d**).

In both examples, the observed b-value changes are likely related to the incompleteness of the catalog in the first period after the mainshock as discussed above. This is also indicated by the lack of small magnitude values in the lower left corner of the plots in Figure **5c,d**.

NW Bohemia swarms

Episodic occurrence of spatially clustered earthquake swarms is well known in the region of West Bohemia/Vogtland, Central Europe, with the most intensive earthquake activity recorded in the years 1896–1897, 1903, 1908–1909, 1985–1986, 2000, and 2008 (Fischer et al., 2014). In contrast to mainshock-aftershock sequences, earthquake swarms are not dominated by a single event. Since 1994, the Novy Kostel area has been monitored by the local seismic network WEBNET, which provides high quality data. A detailed study of the swarm in the year 2000 indicated, among others, that the b-value decreased systematically within the initial swarm period which was interpreted as result of stress accumulation

(Hainzl and Fischer, 2002). Here we repeat this analysis for the 3696 (3133) events with $M \geq 0.3$ occurred during the swarm in the year 2000 (2008). We find that in both cases, a statistically significant drop of the b-value occurred in the initiation phase of the swarm activity. While the b-value remained low afterwards in 2000, it recovers at the end of the swarm activity in the year 2008. Note that in the latter case, the continuous b-value increase suggested by the moving-window approach is again likely a smearing effect due to the fact that the windows still include events from the period with small b-value.

Conclusions

The main objective of this paper is to present an algorithm for the automatic detection of change-points of the Gutenberg-Richter b-value in seismicity data. We use a Bayesian algorithm to identify changes in time. While the detection of a single change-point is straightforward, we have a trade-off between accuracy and computational effort for models with more than one change-point. We have found that an iterative procedure detecting one change point after the other, is a feasible way to find multiple change-points with reasonable effort and sufficient accuracy. It is noteworthy that our method does not require any binning. In contrast, the traditional way to find b-value changes is based on moving windows with given size and time steps leading always to smearing effects. Calculations with synthetic data allow to constrain relations between data, parameters and statistical significances. For example, having an earthquake catalog with given size (say 1000 events) and a predefined error probability (say 5%), we can provide a minimum detectable b-value contrast $\Delta b = b_2 - b_1$ for this situation.

The only assumption of our detection algorithm is the validity of the Gutenberg-Richter law with piecewise constant b-value. Additionally we use prior knowledge about the b-value as explained in Section *Method* and in Section *Test for synthetic data*. Because the b-value is estimated mainly from small earthquakes, potentially missing large events or fluctuations at the right tail of the distribution have almost no influence on the results. However, data errors at the completeness level, e.g. arising from overlapping seismograms in strongly clustered seismicity, might produce misleading results and should therefore be considered with care.

Applying our method to various types of real seismicity like foreshock and aftershock sequences and swarm events, we detect changes of the b-value automatically, regardless of physical mechanisms or potential data artifacts. For the 2014 Iquique earthquake, a foreshock sequence with decreasing b-value has been reported (Schurr et al., 2014). However, a re-evaluation of this case shows that the b-value contrast is too low to accept this change-point with reasonable significance, although the change might be real. On the other hand, examples of the aftershock sequences indicate that detected change-points, although statistically significant, might not always indicate a change of the physical system state, but can be also be related to varying completeness levels in time. This is particularly important in periods of high seismic activity, when the detectability is decreased and earthquake catalogs are typically missing small events (Kagan, 2004; Hainzl, 2016a). Because our method is only based on the magnitude difference, $m = M - M_c$, between the actual magnitude M of an earthquake and the local completeness magnitude M_c at the occurrence time of the event, it can be simply applied to catalogs with time- and space-varying completeness. However, it requires a comprehensive analysis of the completeness level before any search and interpretation of b-value changes.

Finally, we note that b-value changes are often considered to be precursory signals to large earthquakes. This hypothesis is, however, based on specific case studies so far. Our method aims at an automatic detection of such changes and provides a quantitative evaluation of the statistical significance. For this reason, we can expect that it contributes to the design of an objective testing scheme for this potential precursor.

Data and Resources

The aftershock data of the Landers earthquake are from the website *http://scedc.caltech.edu/research-tools/alt-2011-dd-hauksson-yang-shearer.html*, last accessed March 15. 2016.

The foreshocks and aftershocks of the Tohoku earthquake are taken from the JMA catalog from the website *http://www.hinet.bosai.go.jp*, last accessed August 28, 2018.

The foreshock data of the Iquique mainshock and the swarm data are described in publications of Schurr et al. (2014) and Fischer et al. (2014) and are received by contacting the first authors (Bernd Schurr, bernd.schurr@gfz-potsdam.de; Tomas Fischer, fischer@natur.cuni.cz).

Figure **1**, Figure **2**, Figure **3** , Figure **4** and Figure **5** were made using the Gnuplot version

5.2.

Simulations were made using the open source software package Python version 2.7.12.

Acknowledgments

We are grateful to Hannelore Liero for fruitful discussions and comments. The manuscript benefitted from constructive comments of two anonymous reviewers. This work was supported by the DFG Research Training Group "Natural hazards and risks in a changing world"(NatRiskChange). GZ also acknowledges support from the DFG (SFB 1294).

References

Aki, K. (1965). Maximum likelihood estimate of b in the formula log $N = a - bM$ and its confidence limits, *Bull. Earthq. Res. Inst.*, **43**, 237–239.

Amitrano, D. (2003). Brittle-ductile transition and associated seismicity: Experimental and numerical studies and relationship with the b value, *J. Geophys. Res.*, **108**(B1), 2044, doi:10.1029/2001JB000680.

Bachmann, C. E., Wiemer, S., Goertz-Allmann, B. P., and Woessner, J. (2012). Influence of pore-pressure on the event-size distribution of induced earthquakes, *Geophys. Res. Lett.*, **39**, L09302, doi:10.1029/2012GL051480.

Dawid, A. P., Stone, M., and Zidek, J. V. (1973). Marginalization paradoxes in Bayesian and structural inference, *Journal of the Royal Statistical Society. Series B (Methodological)*, 189–233.

Fiedler, B., Zöller, G., Holschneider, M., and Hainzl, S. (2018). Multiple change-point detection in spatio-temporal seismicity data, *Bull. Seismol. Soc. Am.*, **108**(3A): 1147–1159, doi 10.1785/0120170236. .

Fischer, T., Horalek, J., Hrubcova, P., Vavrycuk, V., Bräuer, K., and Kämpf, H. (2014). Intra-continental earthquake swarms in West-Bohemia and Vogtland: A review, *Tectonophysics*, **611**, 1–27.

Goebel,T. H. W., Schorlemmer, D., Becker, T. W., Dresen, G., and Sammis, C. G. (2013). Acoustic emissions document stress changes over many seismic cycles in stick-slip experiments, *Geophys. Res. Lett.*, **40**, 2049–2054, doi:10.1002/grl.50507.

Gutenberg, B., and Richter, C. F. (1956). Earthquake magnitude, intensity, energy, and acceleration (Second paper), *Bull. Seismol. Soc. Am.*, **46**(2), 105–145

Hainzl, S. (2016a). Rate-dependent incompleteness of earthquake catalogs, *Seismol. Res. Lett.*, **87**, 337–344.

Hainzl, S. (2016b). Apparent triggering function of aftershocks resulting from rate-dependent incompleteness of earthquake catalogs, *J. Geophys. Res. Solid Earth*, **121**, 6499–6509, doi:10.1002/2016JB013319.

Hainzl, S., and Fischer, T. (2002). Indications for a successively triggered rupture growth underlying the 2000 earthquake swarm in Vogtland/NW-Bohemia, *J. Geophys. Res.*, **107**(B12), 2338. http://dx.doi.org/10.1029/2002JB001865.

Hauksson, E., Yang, W., and Shearer, P. M. (2012). Waveform relocated earthquake catalog for Southern California (1981 to 2011), *Bull. Seismol. Soc. Am.*, **102**(5), 2239–2244. doi: 10.1785/0120120010

Imoto, M. (1991). Changes in the frequency-magnitude b value prior to large (¿6) earthquakes in Japan, *Tectonophysics*, **193**, 311–325.

Kagan, Y. Y. (2004). Short-term properties of earthquake catalogs and models of earthquake source, *Bull. Seismol. Soc. Am.*, **94**(4), 1207–1228.

Kamer, Y., and Hiemer, S. (2013). Comment on "Analysis of the b-values before and after the 23 October 2011 Mw 7.2 Van-Ercis, Turkey, earthquake" by Ethem Görgün, *Tectonophysics*, **608**, 1448–1451, doi:10.1016/j.tecto.2013.07.040.

Kass, Robert E. and Adrian E. Raftery (1995). Bayes factors, *Journal of the American Statistical Association*, **90**(430), 773–795.

Lopez-Comino, J. A., Cesca, S., Heimann, S., Grigoli, F., Milkereit, C., Dahm, T., and Zang, A. (2017). Characterization of Hydraulic Fractures Growth During the Aspo Hard Rock Laboratory Experiment (Sweden), *Rock Mech. Rock Eng.*, **50**, 2985–3001.

Marzocchi, W., and Sandri, L. (2003). A review and new insights on the estimation of the b-value and its uncertainty, *Ann. Geophys.*, **46**(6), 1271–1282.

Montoya-Noguera, S. and Wang, Y. (2017). Bayesian identification of multiple seismic change points and varying seismic rates caused by induced seismicity, *Geophysical Research Letters*, **44**(8), 3,509–3,516.

Nakaya, S. (2006). Spatiotemporal variation in b value within the subducting slab prior to the 2003 Tokachi-oki earthquake (M 8.0), Japan, *J. Geophys. Res.*, **111**, B03311, doi:10.1029/2005JB003658.

Nanjo, K. Z., Hirata, N., Obara, K., and Kasahara, K. (2012). Decade-scale decrease in b value prior to the M9-class 2011 Tohoku and 2004 Sumatra quakes, *Geophys. Res. Lett.*, **39**, L20304, doi:10.1029/2012GL052997.

Raftery, A. E., and Akman, V. E. (1986). Bayesian analysis of a Poisson process with a change-point, *Biometrika*, **73**(1), 85–89.

Scholz, C. H. (1968). The frequency-magnitude relation of microfracturing in rock and its relation to earthquakes, *Bull. Seismol. Soc. Am.*, **58**, 399–415.

Scholz, C. H. (2015). On the stress dependence of the earthquake b value, *Geophys. Res. Lett.*, **42**, 1399–1402, doi:10.1002/2014GL062863.

Schorlemmer, D., Wiemer, S. and Wyss, M. (2005). Variations in earthquake-size distribution across different stress regimes, *Nature*, **437**(7058), 539.

Schurr, B., G. Asch, S. Hainzl, J. Bedford, A. Hoechner, M. Palo, R. Wang, M. Moreno, M. Bartsch, Y. Zhang, O. Oncken, F. Tilmann, T. Dahm, P. Victor, S. Barrientos, and

J.-P. Vilotte et al. (2014). Gradual unlocking of plate boundary controlled initiation of the 2014 Iquique earthquake, *Nature*, **512**, 299–302.

Shcherbakov, R., Turcotte, D. L., and Rundle, J. B. (2004). A generalized Omori's law for earthquake aftershock decay, *Geophys. Res. Lett.*, **31**, L11613, doi:10.1029/2004GL019808.

Smith, W. D. (1981). The b value as an earthquake precursor, *Nature*, **289**(5794), 136–139.

Spada, M., T. Tormann, S. Wiemer, and B. Enescu (2013). Generic dependence of the frequency-size distribution of earthquakes on depth and its relation to the strength profile of the crust, *Geophys. Res. Lett.*, **40**, 709–714, doi:10.1029/2012GL054198.

Utsu, T., Ogata, Y., and Matsu'ura, R. S. (1995). The centenary of the Omori formula for a decay of aftershock activity, *J. Phys. Earth*, **43**, 1–33.

Wiemer, S. and Wyss, M. (2002). Mapping spatial variability of the frequency-magnitude distribution of earthquakes, *Advances in geophysics. Elsevier*, Vol. 45, 259–V.

Bernhard Fiedler, Institute of Mathematics, University of Potsdam, Karl-Liebknecht-Str. 24-25, 14476 Potsdam, Germany. Email bfiedler@uni-potsdam.de

Sebastian Hainzl, GFZ German Research Centre for Geosciences, Telegrafenberg, 14473 Potsdam, Germany

Gert Zöller, Institute of Mathematics, University of Potsdam, Karl-Liebknecht-Str. 24-

25, 14476 Potsdam, Germany.

Matthias Holschneider, Institute of Mathematics, University of Potsdam, Karl-Liebknecht-Str. 24-25, 14476 Potsdam, Germany.

Figure captions

Figure 1

The estimated probability to erroneously decide for a change-point given in the case of a Bayes-factor $B_{01} < 0.5$. The estimated probability is shown as function of the sample size and color-coded for different b-values of the Gutenberg-Richter distribution. Each point refers to the result for 1000 time series with randomly selected magnitudes from a stationary frequency-magnitude distribution.

Figure 2

The detectability and the precision of detected change-points as function of the number of events and the b-value difference in synthetic sequences. Contour lines are related (**a**) to the estimated probability that the change-point is detected and (**b**) the root-mean-square error of the relative position of detected change-points. The estimations are based on 10,000 synthetic sequences for each parameter set. In all cases, the true change-point is located in the center of the sequence and the average b-value is 1; e.g. the first 500 events are sampled from a Gutenberg-Richter distribution with b_1=0.8 and the second 500 events with $b_2 = 1.2$ for the case of 1000 events with a b-value difference of 0.4.

Figure 3

Analysis of the sensitivity with respect to the prior choice: (**a**) The detectability and (**b**) the precision of the change point as function of the maximum b-value ($\beta_{max}/\ln(10)$) used for the uniformly distributed prior in the interval $[0, b_{max}]$. The results are obtained for $N = 1000$ and three exemplary values of Δb in the synthetic test setup as described in Figure **2**.

Figure 4

Estimated b-values for four types of synthetic sequences including a different number of change-points. For each of them, the magnitude sequence of one example is shown on top, while the resulting b-value estimations for 100 different sequences are shown below as function of the event index. Gray solid lines refer to the iterative procedure using B_{01} and blue dotted lines refer to the procedure using additionally B_{12} to directly decide whether or not two change-points exists. The true b-values are shown in all cases by the red line.

Figure 5

Result of the b-value estimations as function of time for examples of observed seismicity: Foreshock sequences of (**a**) the M8.1 Iquique and (**b**) the M9.0 Tohoku mainshock; aftershock sequences of (**c**) the M7.3 Landers and (**d**) the M9.0 Tohoku mainshock; and earthquake swarms in West Bohemia in the year (**e**) 2000 and (**f**) 2008. In all cases, the recorded magnitudes are shown by gray dots and our resulting b-value estimates are shown in red. For comparison, the maximum likelihood b-value estimate for a moving window of 200 subsequent events with a step size of one are shown in blue. In all cases, the shaded area corresponds to plus/minus one standard deviation.

479 # Figures

480 ## Figure 1

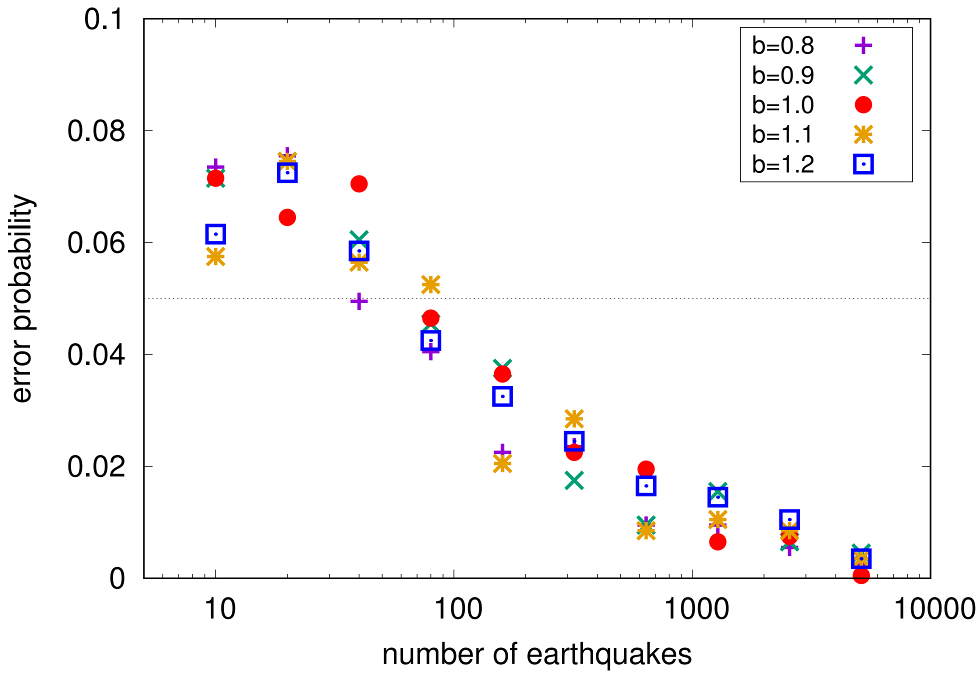

Figure 1: The estimated probability to erroneously decide for a change-point given in the case of a Bayes-factor $B_{01} < 0.5$. The estimated probability is shown as function of the sample size and color-coded for different b-values of the Gutenberg-Richter distribution. Each point refers to the result for 1000 time series with randomly selected magnitudes from a stationary frequency-magnitude distribution.

481 **Figure 2**

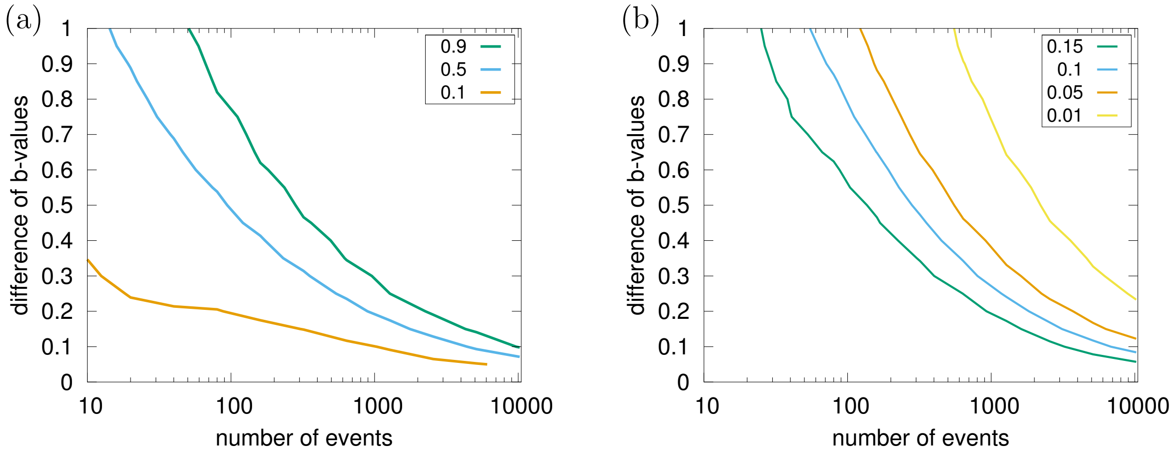

Figure 2: The detectability and the precision of detected change-points as function of the number of events and the b-value difference in synthetic sequences. Contour lines are related (**a**) to the estimated probability that the change-point is detected and (**b**) the root-mean-square error of the relative position of detected change-points. The estimations are based on 10,000 synthetic sequences for each parameter set. In all cases, the true change-point is located in the center of the sequence and the average b-value is 1; e.g. the first 500 events are sampled from a Gutenberg-Richter distribution with b_1=0.8 and the second 500 events with $b_2 = 1.2$ for the case of 1000 events with a b-value difference of 0.4.

Figure 3

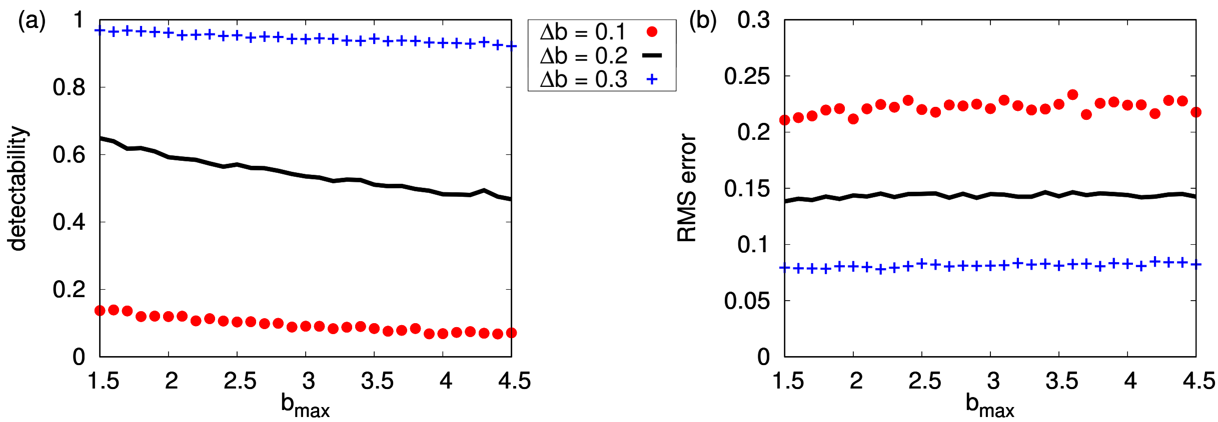

Figure 3: Analysis of the sensitivity with respect to the prior choice: (**a**) The detectability and (**b**) the precision of the change point as function of the maximum b-value ($\beta_{max}/\ln(10)$) used for the uniformly distributed prior in the interval $[0, b_{max}]$. The results are obtained for $N = 1000$ and three exemplary values of Δb in the synthetic test setup as described in Figure **2**.

483 Figure 4

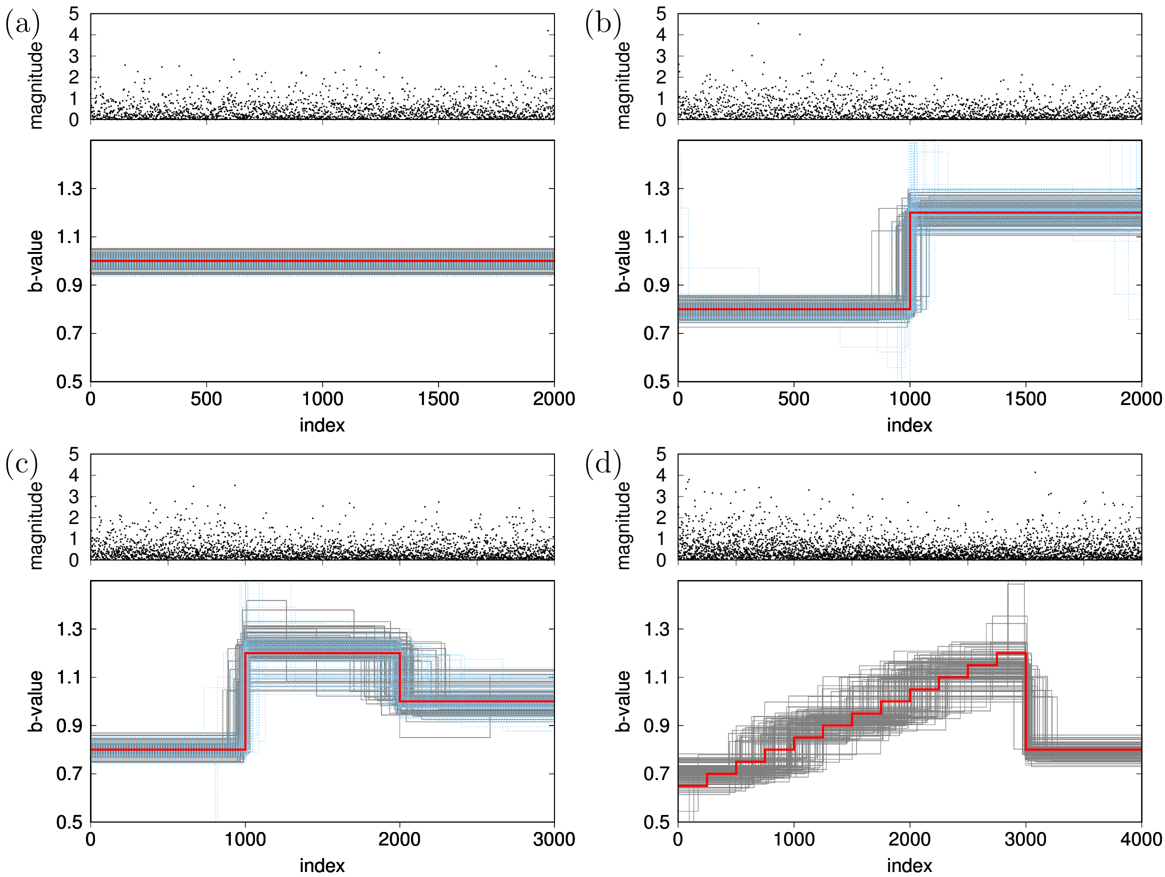

Figure 4: Estimated b-values for four types of synthetic sequences including a different number of change-points. For each of them, the magnitude sequence of one example is shown on top, while the resulting b-value estimations for 100 different sequences are shown below as function of the event index. Gray solid lines refer to the iterative procedure using B_{01} and blue dotted lines refer to the procedure using additionally B_{12} to directly decide whether or not two change-points exists. The true b-values are shown in all cases by the red line.

Figure 5

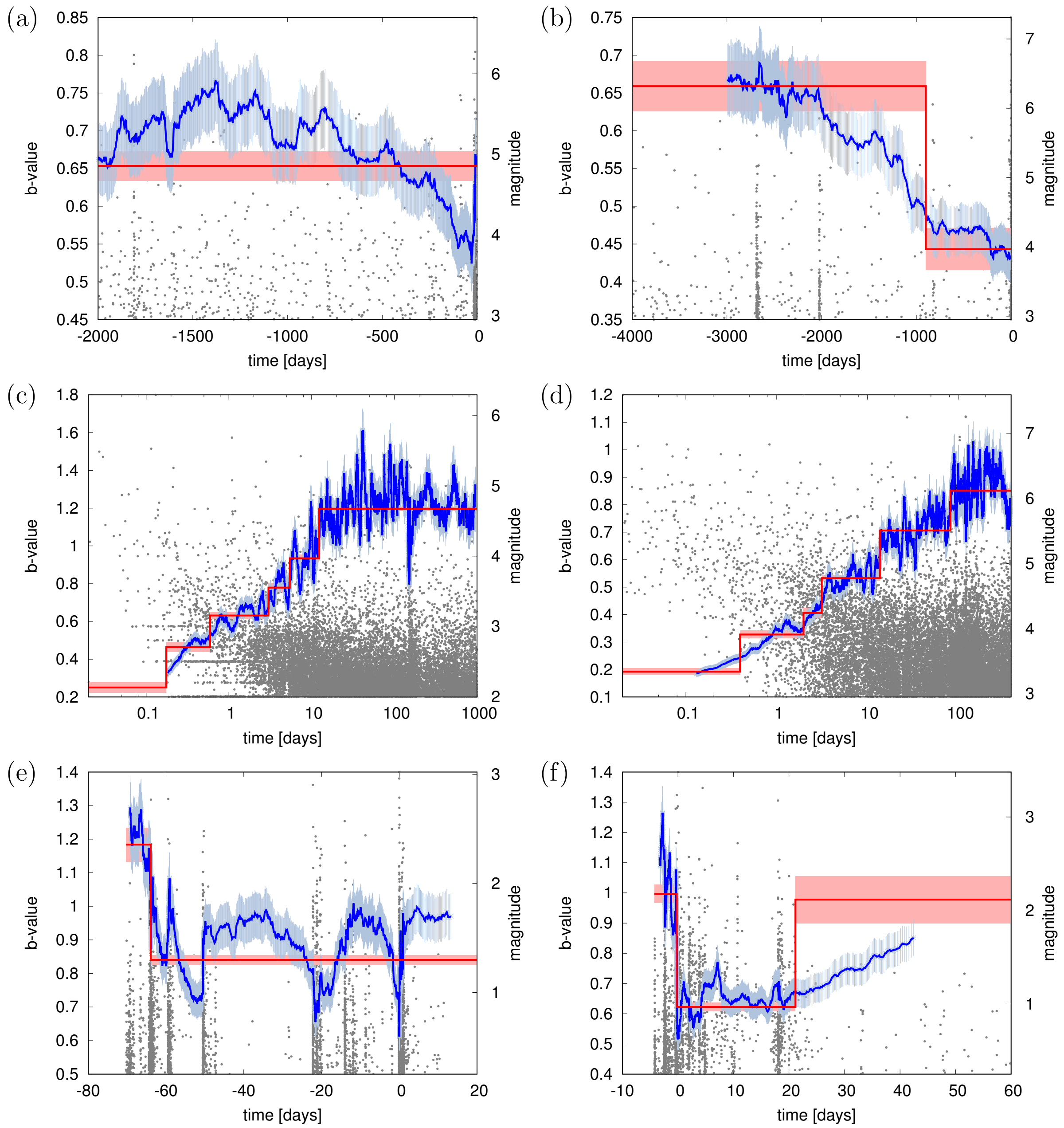

Figure 5: Result of the b-value estimations as function of time for examples of observed seismicity: Foreshock sequences of (**a**) the M8.1 Iquique and (**b**) the M9.0 Tohoku mainshock; aftershock sequences of (**c**) the M7.3 Landers and (**d**) the M9.0 Tohoku mainshock; and earthquake swarms in West Bohemia in the year (**e**) 2000 and (**f**) 2008. In all cases, the recorded magnitudes are shown by gray dots and our resulting b-value estimates are shown in red. For comparison, the maximum likelihood b-value estimate for a moving window of 200 subsequent events with a step size of one are shown in blue. In all cases, the shaded area corresponds to plus/minus one standard deviation.

Appendix

Appendix: Derivation of Bayes-factors

Using a uniform prior for β within $[0, \beta_{max}]$, i.e. $p(\beta) = \beta_{max}^{-1}$, and a discrete uniform prior distribution for the change-point position k, that is $p(k) = \frac{1}{N-1}$, Eq. (9) becomes

$$\begin{aligned} p(\underline{m} \mid \mathcal{M}_0) &= \int\limits_0^{\beta_{max}} \frac{1}{\beta_{max}} \beta^N \exp\left(-\beta \sum_{i=1}^{N} m_i\right) d\beta \\ &= \frac{1}{\beta_{max}} \left[\sum_{i=1}^{N} m_i\right]^{-(N+1)} \gamma\left(N+1, \beta_{max} \sum_{i=1}^{N} m_i\right). \end{aligned} \tag{A1}$$

Here

$$\gamma(l, c) = \int\limits_0^{c} x^{l-1} \exp(-x)\, dx \tag{A2}$$

denotes the incomplete gamma function. Further Eq. (10) becomes

$$\begin{aligned} p(\underline{m} \mid \mathcal{M}_1) &= \frac{\beta_{max}^{-2}}{N-1} \sum_{k=1}^{N-1} \int\limits_0^{\beta_{max}} \int\limits_0^{\beta_{max}} \beta_1^k \exp\left(-\beta_1 \sum_{i=1}^{k} m_i\right) \beta_2^{N-k} \exp\left(-\beta_2 \sum_{i=k+1}^{N} m_i\right) d\beta_1\, d\beta_2 \\ &= \frac{\beta_{max}^{-2}}{N-1} \sum_{k=1}^{N-1} \left\{ \left[\sum_{i=1}^{k} m_i\right]^{-(k+1)} \gamma\left(k+1, \beta_{max} \sum_{i=1}^{k} m_i\right) \right. \\ &\quad \left. \times \left[\sum_{i=k+1}^{N} m_i\right]^{-(N-k+1)} \gamma\left(N-k+1, \beta_{max} \sum_{i=k+1}^{N} m_i\right) \right\}. \end{aligned} \tag{A3}$$

Hence the resulting Bayes factor B_{01} is given by

$$B_{01} = \frac{\beta_{max}(N-1) \left[\sum\limits_{i=1}^{N} m_i\right]^{-(N+1)} \gamma\left(N+1, \beta_{max} \sum\limits_{i=1}^{N} m_i\right)}{\sum\limits_{k=1}^{N-1} \left\{ \left[\sum\limits_{i=1}^{k} m_i\right]^{-(k+1)} \gamma\left(k+1, \beta_{max} \sum\limits_{i=1}^{k} m_i\right) \left[\sum\limits_{i=k+1}^{N} m_i\right]^{-(N-k+1)} \gamma\left(N-k+1, \beta_{max} \sum\limits_{i=k+1}^{N} m_i\right) \right\}} \tag{A4}$$

Similarly, the Bayes factor for two change-points B_{02} is derived by calculating $p(\underline{m} \mid \mathcal{M}_2)$ with the same prior assumptions for $\beta_i,\ i = 1, 2, 3$ as in Eq. (A3). Further let $\underline{k} = \{k_1, k_2\}$ with $k_1 < k_2$ be the positions of the change-points and we assume that k is uniformly distributed over all possible partitions. Hence the prior density of k becomes

$$p(\underline{k}) = \left[\binom{N-1}{2}\right]^{-1}. \tag{A5}$$

Therefore we get

$$\begin{aligned}
p(\underline{m} \mid \mathcal{M}_2) &= \frac{2\beta_{max}^{-3}}{(N-1)(N-2)} \sum_{k_1=1}^{N-1} \sum_{k_2=k_1+1}^{N-1} \int_0^{\beta_{max}} \int_0^{\beta_{max}} \int_0^{\beta_{max}} \beta_1^{k_1} \exp\left(-\beta_1 \sum_{i=1}^{k_1} m_i\right) \beta_2^{k_2-k_1} \\
&\times \exp\left(-\beta_2 \sum_{i=k_1+1}^{k_2} m_i\right) \beta_3^{N-k_2} \exp\left(-\beta_2 \sum_{i=k_2+1}^{N} m_i\right) d\beta_1\, d\beta_2\, d\beta_3 \\
&= \frac{2\beta_{max}^{-2}}{(N-1)(N-2)} \sum_{k_1=1}^{N-1} \sum_{k_2=k_1+1}^{N-1} \left\{ \left[\sum_{i=1}^{k_1} m_i\right]^{-(k_1+1)} \gamma\left(k_1+1, \beta_{max} \sum_{i=1}^{k_1} m_i\right) \right. \\
&\times \left[\sum_{i=k_1+1}^{k_2} m_i\right]^{-(k_2-k+1)} \gamma\left(k_2-k_1+1, \beta_{max} \sum_{i=k_1+1}^{k_2} m_i\right) \\
&\times \left. \left[\sum_{i=k_1+1}^{N} m_i\right]^{-(N-k_2+1)} \gamma\left(N-k_2+1, \beta_{max} \sum_{i=k_2+1}^{N} m_i\right) \right\}.
\end{aligned} \tag{A6}$$

Using Eq. (A1), Eq. (A3) and Eq. (A6) we can calculate B_{02} and B_{12} by

$$B_{02} = \frac{p(\underline{m} \mid \mathcal{M}_0)}{p(\underline{m} \mid \mathcal{M}_2)} \tag{A7}$$

and

$$B_{12} = \frac{p(\underline{m} \mid \mathcal{M}_1)}{p(\underline{m} \mid \mathcal{M}_2)}. \tag{A8}$$

Estimation of multiple change-points

In the following we show the extension of our methodology from Section *Estimation of change-points*. We again consider an observation period of $[T_0,\ T_1]$ with N events at times

$$T_0 \leq t_1 < t_2 < \ldots < t_N \leq T_1. \tag{A9}$$

Here m_i is the magnitude occurring at time t_i, $i = 1, \ldots, N$. We assume the existence of n change-points at location

$$k_1,\ k_2,\ \ldots,\ k_n \in \{1, \ldots,\ N-1\} \tag{A10}$$

with $n < N$. Moreover in $[T_0,\ t_{k_1}]$ we have k_1 events with Gutenberg-Richter value β_1 and $k_i - k_{i-1}$ events in $(t_{k_{i-1}},\ t_{k_i}]$ with Gutenberg-Richter value β_i for $i = 2,\ \ldots,\ n$. Finally, in $[t_{k_n},\ T_1]$ the number of events is $N - k_n$ with Gutenberg-Richter value β_{n+1} .

Let $\underline{m} = \{m_1, \ldots, m_N\}$ and $\theta = \{\beta_1,\ \ldots,\ \beta_{n+1},\ k_1,\ \ldots,\ k_n\}$. It can easily be shown that the mutual likelihood function is given by

$$\begin{aligned} p(\underline{m} \mid \theta) &= \beta_1^{k_1} \exp\left(-\beta_1 \sum_{i=1}^{k_1} m_i\right) \ldots \beta_{n+1}^{N-k_n} \exp\left(-\beta_{n+1} \sum_{i=k_n+1}^{N} m_i\right) \\ &= \beta_1^{k_1} \exp\left(-\beta_1 \sum_{i=1}^{k_1} m_i\right) \beta_{n+1}^{N-k_n} \exp\left(-\beta_{n+1} \sum_{i=k_n+1}^{N} m_i\right) \\ &\quad \times \prod_{j=2}^{n} \beta_j^{k_j - k_{j-1}} \exp\left(-\beta_j \sum_{l=k_{j-1}+1}^{k_j} m_l\right). \end{aligned} \tag{A11}$$

Assuming for simplicity now a flat prior, we calculate the marginal posterior density of $\underline{k} = \{k_1,\ \ldots,\ k_n\}$ by integrating with respect to $\beta_1,\ \ldots,\ \beta_{n+1}$.

$$\begin{aligned}
p(\underline{k} \mid \underline{m}) &= c \int_0^\infty \ldots \int_0^\infty \beta_1^{k_1} \exp\left(-\beta_1 \sum_{i=1}^{k_1} m_i\right) \beta_{n+1}^{N-k_n} \exp\left(-\beta_{n+1} \sum_{i=k_n+1}^{N} m_i\right) \\
&\qquad \times \prod_{j=2}^{n} \beta_j^{k_j-k_{j-1}} \exp\left(-\beta_j \sum_{l=k_{j-1}+1}^{k_j} m_l\right) d\beta_1 \ldots d\beta_{n+1} \\
&= c \left[\sum_{i=1}^{k_1} m_i\right]^{-(k_1+1)} \Gamma(k_1+1) \left[\sum_{i=k_n+1}^{N} m_i\right]^{-(N-k_n+1)} \Gamma(N-k_n+1) \\
&\qquad \times \prod_{j=2}^{n} \left[\sum_{l=k_{j-1}+1}^{k_j} m_l\right]^{-(k_j-k_{j-1}+1)} \Gamma(k_j-k_{j-1}+1).
\end{aligned} \tag{A12}$$

We note that in Eq. (A12) c is a normalizing constant which ensures that the conditions for a probability density function is fulfilled.